Ke-Chang Hung and Jyh-Horng Wu*

Comparison of physical and thermal properties of various wood-inorganic composites (WICs) derived by the sol-gel process

https://doi.org/10.1515/hf-2017-0156
Received September 27, 2017; accepted December 18, 2017; previously published online January 17, 2018

Abstract: The physical properties and thermal decomposition kinetics of wood-inorganic composites (WICs) were in focus, which were prepared from methyltriethoxysilane (MTEOS), tetraethoxysilane (TEOS) and titanium (IV) isopropoxide (TTIP) by the sol-gel process. The hydrophobicity and dimensional stability of the composites were better than those of unmodified wood (W_{contr}), but the performance of SiO_2-based WICs (WIC_{SiO_2}) was the best. The SEM-EDX micrographs show that silica is only distributed within the cell wall of the WIC_{SiO_2}. By contrast, titania was deposited principally in the cell lumens of the WIC_{TiO_2}. The thermal decomposition kinetic experiments show that the average apparent activation energies with conversion rates between 10% and 70% were 156–168 (W_{contr}), 178–180 (WIC_{MTEOS}), 198–214 (WIC_{TEOS}) and 199–204 (WIC_{TTIP}) kJ mol^{-1} at the impregnation level of 20% weight gain. The reaction order values calculated based on the Avrami theory were 0.51–0.57, 0.39–0.51, 0.36–0.47 and 0.28–0.51 in the same order of species indicated above. Accordingly, the dimensional and thermal stability of the wood could be enhanced effectively by the sol-gel process with silicon- and titanium-based alkoxides.

Keywords: activation energy, dimensional stability, methyltriethoxysilane (MTEOS), model-free isoconversional methods, reaction order, sol-gel process, tetraethoxysilane (TEOS), thermal decomposition kinetics, thermal stability, titanium (IV) isopropoxide (TTIP), wood-inorganic composites (WICs)

***Corresponding author: Jyh-Horng Wu,** Department of Forestry, National Chung Hsing University, Taichung 402, Taiwan, Phone: +886 4 22840345, Fax: +886 4 22851308, e-mail: eric@nchu.edu.tw
Ke-Chang Hung: Department of Forestry, National Chung Hsing University, Taichung 402, Taiwan

Introduction

Some properties of wood (dimensional instability, biodeterioration, weathering and flammability) limit wood's outdoor application (Saka and Ueno 1997; Li et al. 2011). Over the past six decades, several wood modifications were developed including acetylation, furfurylation, propionylation, heat treatment and inorganic modification by sol-gel technology (Hill 2006; Wang et al. 2012; Pries and Mai 2013; Himmel and Mai 2016; Moghaddam et al. 2016; Beck et al. 2018a,b). The sol-gel-derived wood-inorganic composites (WICs) are considered to have a high potential to obtain value added and improved products (Sakka and Miyafuji 2005; Tshabalala et al. 2011; Shabir Mahr et al. 2012, 2013; Gholamiyan et al. 2016). The first study in this context was done by Saka et al. (1992). Since that time, numerous investigations have proven that WIC_{SiO_2} prepared by the sol-gel process has an improved flame retardancy, UV stability and fungal resistance (Kartal et al. 2004; Tshabalala et al. 2011; Qin and Zang 2012; Wang et al. 2012). To describe the thermal decomposition behavior of the polymer materials and natural fibers, the activation energy is one of the important parameters (Yao et al. 2008; Poletto et al. 2012; Li et al. 2013; Zhang et al. 2016; Bartocci et al. 2017). Usually, the quality check of WIC is done by differential scanning calorimetry (DSC) and thermogravimetric analysis (TGA) (Saka and Ueno 1997; Shabir Mahr et al. 2012; Wang et al. 2012; Ma et al. 2015; Chandrasekaran et al. 2017; Hung et al. 2017; Lee et al. 2017; Strandberg et al. 2017). Hung and Wu (2017) applied first this technique for WIC_{SiO_2} and found that the activation energy of the thermal decomposition can be effectively enhanced by methyltrimethoxysilane treatment. However, the influence of different metal alkoxides on the physical properties and thermal decomposition of the WICs is still not clear.

The objective of the present paper is to fill this gap. WICs should be prepared via the sol-gel process, which are based on treatments with methyltriethoxysilane (MTEOS), tetraethoxysilane (TEOS) and titanium (IV) isopropoxide (TTIP), and their physical and thermal properties should be characterized.

Materials and methods

Japanese cedar (*Cryptomeria japonica* D. Don) sapwood (20–30 years old) was supplied by the experimental forest of National Taiwan University. The dimensions of slicewood samples were 3 mm (R) × 12 mm (T) × 58 mm (L). The oven-dried (o.d.) wood specimens selected for this study were free of defects and exhibited a modulus of elasticity from 8.0 to 9.0 GPa. The samples were investigated after extraction in a Soxhlet apparatus for 24 h with a 1:2 (v/v) mixture of ethanol and toluene, followed by washing with distilled water. The extracted slicewood samples were oven-dried at 105°C for 12 h, and their weights were measured. The WIC_{TiO_2} samples were made of the o.d. wood. Wood was conditioned at 20°C/65% RH for 1 week prior to the preparation of WIC_{MTEOS}, WIC_{TEOS} and WIC_{TTIP}. The chemicals were purchased from Acros Chemical (Geel, Belgium). The other chemicals and solvents used in this experiment were of the highest quality.

Preparation of WICs: The precursor sol was formulated with reagents (MTEOS, TEOS or TTIP), solvents (methanol or 2-propanol) and acetic acid at a molar ratio of 0.12/1/0.08, respectively, for preparing the composites. The wood specimens were impregnated with the prepared sol under reduced pressure for 3 days. The impregnated specimens were then heated to 50°C for 24 h and 105°C for another 24 h to age the gels (Miyafuji et al. 2004). The weight percent gain (WPG) was determined based on the o.d. weights.

Determination of physical properties: Density, moisture content (MC) and water absorption (WA) and volume swelling (VS) tests were carried out according to ASTM (D1037-06a 2006; D2395-07a 2007; D4442-07 2007), respectively. Five specimens for each WIC were conditioned at 20°C/65% RH for 2 weeks before testing.

Scanning electron microscopy (SEM): The bending fractured wood and WICs were cut with a microtome knife on the transverse surface, and block specimens [3 mm (R) × 3 mm (T) × 2 mm (L)] were obtained. The instrument (SEM-EDX, JEOL JSM-6330F, Tokyo, Japan) was equipped with an energy-dispersive X-ray analysis (EDX) device. The dried specimens were taped on circular holders and coated with platinum for SEM-EDX. The samples were imaged at 3.0 kV.

Thermogravimetric analysis (TGA): A Perkin Elmer Pyris 1 instrument was used (Shelton, USA). All the samples were dried at 105°C for 12 h before TGA. The tests on a 3-mg sample were carried out in a nitrogen atmosphere (20 ml min^{-1}) from 50 to 600°C at heating rates of 5, 10, 20, 30 and 40°C min^{-1}. The kinetic parameters were calculated based on the data obtained by isoconversional methods. The conversion rate α is defined:

$$\alpha = \frac{W_0 - W_t}{W_0 - W_f} \tag{1}$$

where W_0 is the initial weight of the sample, W_f is the final residual weight and W_t is the weight of the oxidized or pyrolyzed sample at time t. The common isoconversional methods used in this study include the methods according to Friedman (Eq. 2), Flynn-Wall-Ozawa (F-W-O) (Eq. 3), modified Coats-Redfern (modified C-R) (Eq. 4) and Starink (Eq. 5):

$$\ln\frac{d\alpha}{dt} = \ln[Af(\alpha)] - \frac{E_a}{RT} \tag{2}$$

$$\log\beta = \log\frac{AE_a}{Rg(\alpha)} - 2.315 - 0.4567\frac{E_a}{RT} \tag{3}$$

$$\ln\frac{\beta}{T^2\left(1-\frac{2RT}{E_a}\right)} = \ln\frac{-AR}{E_a\ln(1-\alpha)} - \frac{E_a}{RT} \tag{4}$$

$$\ln\frac{\beta}{T^{1.8}} = C_s - 1.0037\frac{E_a}{RT} \tag{5}$$

where α is the conversion rate, A is the pre-exponential factor (min^{-1}), $f(\alpha)$ is the reaction model, E_a is the apparent activation energy (kJ mol^{-1}), R is the gas constant (8.314 J K^{-1} mol^{-1}), T is the absolute temperature (K), β is the heating rate, $g(\alpha)$ is a function of the conversion and C_s is a constant (Yao et al. 2008; Gai et al. 2013; Li et al. 2013). Therefore, for a given conversion, linear relationships are observed by plotting $\ln(d\alpha/dt)$, $\log\beta$, $\ln(\beta/T^2)$ and $\ln(\beta/T^{1.8})$ vs. $1/T$ at different heating rates; the E_a is calculated from the slope of the straight line.

In addition to E_a, the reaction order is also an important parameter of thermal decomposition of wood (Gai et al. 2013). The reaction order in this study is given by the Avrami theory (Eq. 6) as follows:

$$\ln[-\ln(1-\alpha)] = \ln A - \frac{E_a}{RT} - n\ln\beta \tag{6}$$

where n represents the reaction order. For a given temperature, a linear relationship is observed by plotting $\ln[-\ln(1-\alpha)]$ vs. $\ln\beta$ at different temperature heating rates, and the reaction order is deduced from the slope of the line (Gai et al. 2013).

Analysis of variance: All results are expressed in terms of the mean ± SD. The significance of the differences was calculated based on the Scheffe's test; P-values <0.05 are considered significant.

Results and discussion

Physical properties of WICs

The physical properties of WIC_{MTEOS}, WIC_{TEOS} and WIC_{TTIP} with WPGs of 20% are listed in Table 1. Accordingly, the densities of all samples ranged from 440 to 532 kg m^{-3}, and the MCs of the WICs are significantly lower than that of untreated wood (W_{contr}). After 24 h of water immersion, the WA and VS of the WICs are significantly better than the corresponding data of W_{contr}, while the latter disposes of 96% WA and 9.3% VS. These data are decreased for WICs to 43–76% and 3.7–5.4%, respectively. This is due to the deposition and coating with the indicated compounds on the cell walls, cell lumens and intercellular spaces leading to hydrophobization (Kartal et al. 2009; Tshabalala et al. 2011).

Table 1: Physical properties of W_{contr} and WICs.

Specimen	WPG (%)	Density (kg m^{-3})	MC (%)	24 h soaking	
				WA (%)	VS (%)
W_{contr}	–	440 ± 7^{c}	9.3 ± 0.3^{a}	96 ± 9^{a}	9.3 ± 2.3^{a}
WIC_{MTEOS}	20 ± 1^{a}	$479 \pm 23^{b,c}$	7.1 ± 0.1^{d}	43 ± 2^{c}	3.9 ± 0.7^{b}
WIC_{TEOS}	21 ± 2^{a}	$520 \pm 43^{a,b}$	8.3 ± 0.1^{c}	66 ± 8^{b}	3.7 ± 0.7^{b}
WIC_{TTIP}	20 ± 1^{a}	532 ± 6^{a}	8.9 ± 0.1^{b}	76 ± 7^{b}	5.4 ± 0.5^{b}

Values are presented as mean ± SD ($n = 5$). Different superscript letters within a column indicate a significant difference at $P < 0.05$. WA, Water absorption; VS, volume swelling; MC, moisture content.

Figure 1 shows cross-sectional SEM-EDX mappings. Only a few signals (background noise) from the silicon (Figure 1a) and titanium (Figure 1d) are visible in case of W_{contr}. In cases of WIC_{MTEOS} (Figure 1b) and WIC_{TEOS} (Figure 1c), however, SiO_2 was seen within the cell walls. Sakka and Miyafuji (2005) made similar observations. In the course of sol-gel process, hydrolysis reaction of the silicon alkoxides occurs with water, and polycondensation reactions take place. Therefore, the silicon distribution is also influenced by the water-retaining condition in the cell wall, i.e. the silicon location truly reflects the spatial MC distribution. By contrast, in the WIC_{TTIP}, the titanium is only deposited in the cell lumens (Figure 1e) in o.d. wood specimens. The hydrolysis rate of titanium alkoxides is faster than that of the silicon alkoxides (Saka and Yakake 1993; Hübert et al. 2010), and thus, the hydrolysis and condensation reactions of TTIP occur in the cell lumens before the cell wall penetration. Clearly, dimensional stability can only be effectuated by reactive agents in the cell wall; those in the cell lumens play only a minor role (Wang et al. 2012). This is the reason why the performance of WIC_{MTEOS} and WIC_{TEOS} is better than that of WIC_{TTIP}.

Thermal properties of WICs

The TGA curves in Figure 2 illustrate the gradually increased weight loss (WL) above 200°C in case of W_{contr}, and the WL_{max} around 350°C. As known, the thermally instable hemicelluloses are mainly responsible for the initial phase of degradation (Boonstra and Tjeerdsma 2006; Chaouch et al. 2010; Wang et al. 2012). The thermal degradation reactions of WICs are retarded by ca. 10°C. Similar results were obtained by Saka and Ueno (1997), Miyafuji and Saka (2001) and Wang et al. (2012). Additionally, the solid residues of all WICs (23.1–31.1%) are higher than W_{contr} (18.3%) at 600°C, i.e. the deposited SiO_2 or TiO_2 increased the charcoal yield (Rowell and LeVan-Green 2005; Hung and Wu 2017).

The model-free isoconversional method was also applied to TG data evaluation. The plots of the methods according to isoconversional Friedman, F-W-O, modified C-R and Starink show the general trend in the E_a evolution (Figure 3). The E_a is defined as the minimum energy required to overcome the energy barrier in a chemical reaction (Gao et al. 2016). The slopes of the fitted lines

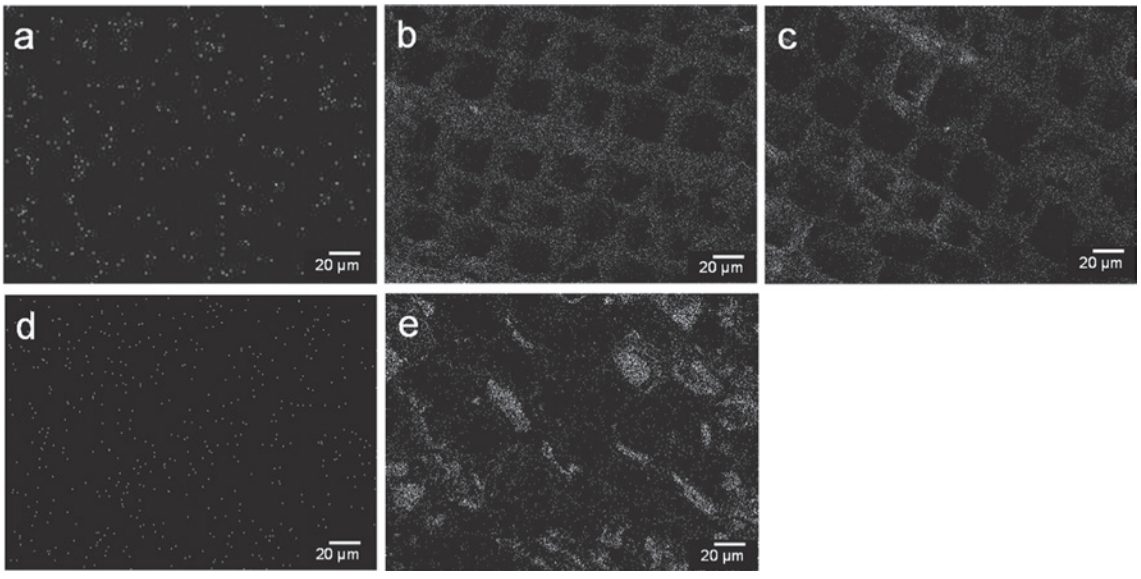

Figure 1: Cross-sectional SEM-EDX mappings.
The cross-sectional micrographs of SEM-EDX elemental mapping of various WICs obtained with WPGs of 20%: (a) W_{contr} (Si mapping); (b) WIC_{MTEOS} (Si mapping); (c) WIC_{TEOS} (Si mapping); (d) W_{contr} (Ti mapping); and (e) WIC_{TTIP} (Ti mapping).

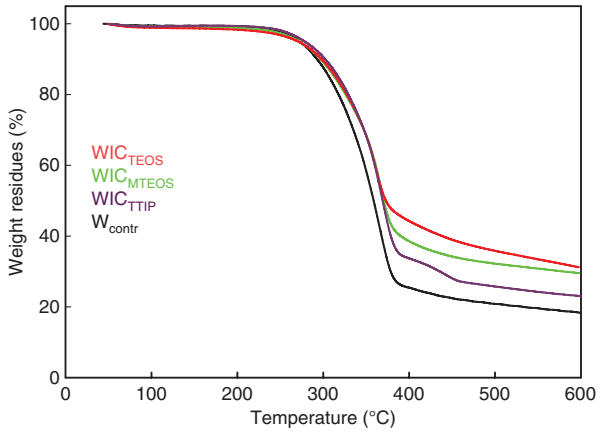

Figure 2: Thermogravimetric curves of W_{contr} and WICs with WPG 20% prepared from different metal alkoxides.

at conversion rates between 10% and 70% were almost parallel, indicating a similar E_a at different conversions. The plots of all WICs have similar trends (the WIC_{MTEOS} and WIC_{TEOS} plots are not shown). As found by Yao et al. (2008), the E_a values are always very similar nearly independently from the conversion rates. It is possible that a single reaction mechanism governs the decomposition (or a stable combination of multiple reaction mechanisms). The apparent activation energy E_a was estimated in the conversion range of 10–70%, which are compiled together with the correlation coefficients (R^2) in Table 2.

In Table 2, the average E_a value of W_{contr} is 168 kJ mol^{-1} according to Friedman for the conversion rates of 10 – 70%. Yao et al. (2008) reported on average E_a values of 156.0 and 161.5 kJ mol^{-1} for maple and pine, respectively, according to Friedman (for conversion rates of 10–60%). The average E_a values are 178, 214 and 199 kJ mol^{-1} of the WIC_{MTEOS}, WIC_{TEOS} and WIC_{TTIP}, respectively. In summary, the minimum energy required to start the thermal decomposition was increased in WICs. The results obtained from the F-W-O, modified C-R and Starink methods also confirm this observation (Table 2). The average E_a values for the conversion range 10–70% are 156–158 (W_{contr}), 179–180 (WIC_{MTEOS}), 198 (WIC_{TEOS}) and 204 (WIC_{TTIP}) kJ mol^{-1}. Brown et al. (2000) and Yao et al. (2008) stated that different kinetic analysis methods are complementary rather than competitive. Therefore, a suitable E_a range could be obtained by combining all observations in Table 2. Interestingly, the average E_a values of WIC_{MTEOS} are significantly lower than those of WIC_{TEOS} and WIC_{TTIP}. According to Chi (1983), MTEOS derived gel is almost uniquely composed

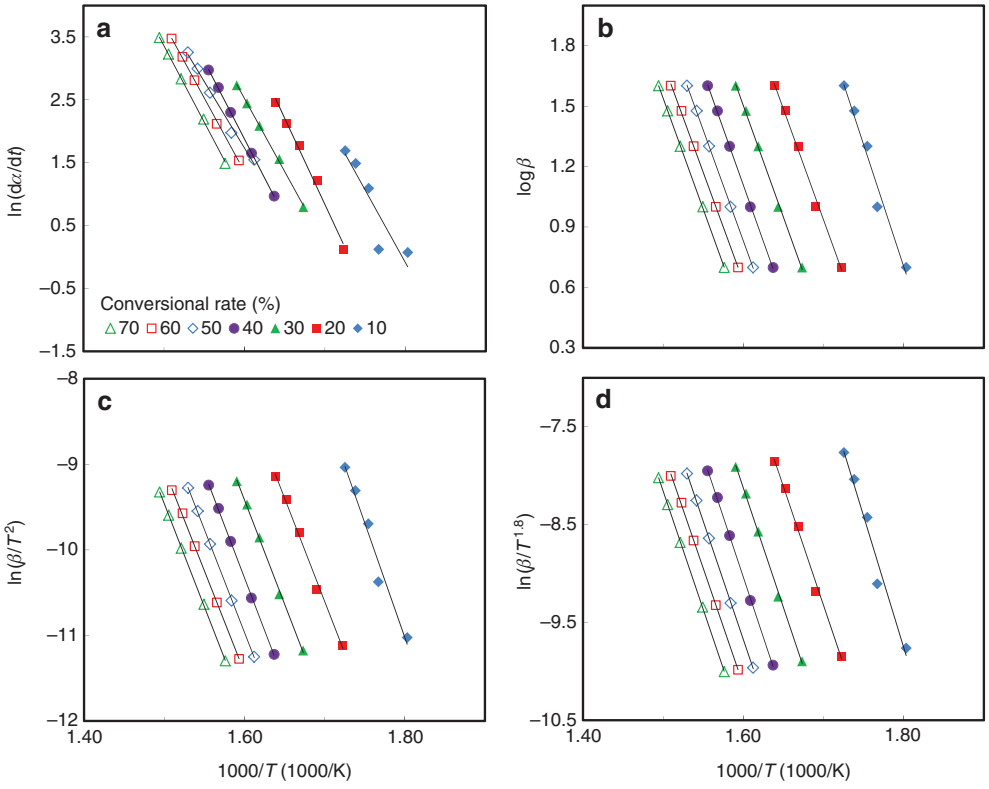

Figure 3: The plots of the methods according to isoconversional Friedman, F-W-O, modified C-R and Starink show the general trend in the E_a evolution.
Typical isoconversional plots prepared based on the methods of Friedman (a), F-W-O (b), modified C-R (c) and Starink (d) concerning WIC_{TTIP}.

Table 2: Apparent activation energy and reaction order of W_{contr} and WICs (WPG 20%) calculated based on the Friedman, F-W-O, modified C-R and Starink methods and the Avrami theory.

Specimen, Methods	E_a(kJ mol^{-1}), Reac. order, R^2	Conversion rates							
		10%	20%	30%	40%	50%	60%	70%	Mean
W_{contr}									
Friedman	E_a	175	159	164	161	169	173	172	168
	R^2	0.998	0.997	~1	0.993	~1	0.997	0.999	–
F-W-O	E_a	149	153	155	159	162	164	167	158
	R^2	0.981	0.991	0.993	0.995	0.997	0.998	0.998	–
Modified C-R	E_a	147	152	153	157	160	162	165	156
	R^2	0.979	0.990	0.993	0.994	0.996	0.998	0.998	–
Starink	E_a	148	152	154	158	160	162	165	157
	R^2	0.979	0.990	0.993	0.994	0.996	0.998	0.998	–
Avrami theory	Reac. order	0.53	0.52	0.51	0.51	0.51	0.53	0.57	0.53
	R^2	0.955	0.989	0.992	0.994	0.994	0.991	0.991	–
WIC_{MTEOS}									
Friedman	E_a	187	178	195	184	171	163	170	178
	R^2	0.999	0.999	0.988	0.996	0.997	0.995	0.980	–
F-W-O	E_a	178	178	182	185	182	179	176	180
	R^2	0.994	0.996	0.996	0.996	0.996	0.995	0.994	–
Modified C-R	E_a	178	178	181	184	180	177	175	179
	R^2	0.993	0.995	0.996	0.995	0.995	0.994	0.993	–
Starink	E_a	178	178	181	184	181	178	175	180
	R^2	0.993	0.995	0.996	0.995	0.995	0.994	0.993	–
Avrami theory	Reac. order	0.40	0.42	0.41	0.39	0.40	0.45	0.51	0.43
	R^2	0.991	0.994	0.993	0.994	0.999	0.999	0.994	–
WIC_{TEOS}									
Friedman	E_a	185	196	217	199	199	212	291	214
	R^2	0.955	0.988	0.996	0.997	~1	0.998	0.975	–
F-W-O	E_a	179	188	194	201	200	203	220	198
	R^2	0.999	~1	~1	~1	~1	~1	0.997	–
Modified C-R	E_a	179	188	194	201	200	203	221	198
	R^2	0.999	~1	~1	~1	~1	~1	0.997	–
Starink	E_a	180	188	194	201	201	203	221	198
	R^2	0.999	~1	~1	~1	~1	~1	0.997	–
Avrami theory	Reac. order	0.36	0.39	0.39	0.39	0.40	0.44	0.47	0.41
	R^2	0.999	0.999	0.999	~1	0.998	0.996	0.998	–
WIC_{TTIP}									
Friedman	E_a	192	228	193	206	176	195	202	199
	R^2	0.825	0.989	0.999	~1	0.991	0.999	0.999	–
F-W-O	E_a	220	201	202	203	201	198	200	204
	R^2	0.973	0.995	0.999	~1	~1	~1	~1	–
Modified C-R	E_a	222	201	202	204	200	197	200	204
	R^2	0.971	0.995	0.999	~1	~1	~1	~1	–
Starink	E_a	223	201	203	204	201	198	200	204
	R^2	0.971	0.995	0.999	~1	~1	~1	~1	–
Avrami theory	Reac. order	0.28	0.34	0.37	0.38	0.41	0.46	0.51	0.39
	R^2	0.932	0.987	0.998	0.998	0.996	0.992	0.992	–

of Si-O network and CH_3 groups with a composition of $CH_3SiO_{3/2}$. In air, the CH_3 groups are removed at 400–600°C and leave behind Si-OH bonds in the -Si-O-Si- backbone (Kamiya et al. 1990; Innocenzi et al. 1994). In an inert atmosphere (N_2 or He), however, the Si-CH_3 bonds are thermally cracked around 600–700°C (Kamiya et al. 1990; Nocuń et al. 2005). No organics evolution was noticed below 600°C for both TEOS and TTIP derived gels, except for the desorption of physisorbed and chemically bonded water (Yoon et al. 2003; Zaharescu et al. 2003). In the present study, TGA was carried out in N_2 between 50°C and 600°C, and the E_a value of WIC_{MTEOS} was lower than

that of WIC_{TEOS}. Zaharescu et al. (2003) reported that the MTEOS-derived gel contains more unhydrolyzed $-OC_2H_5$ groups compared to TEOS-based gel, and the residual $-OC_2H_5$ groups were thermally removed as ethylene and methane at around 560°C as maximum removal rate in an inert atmosphere. In summary, TEOS- and TTIP-based composites have a higher thermal stability than MTEOS-based composites, and this could be explained that more stable crack-free gels are localized in their wood matrix in case of WIC_{TEOS} and WIC_{TTIP}. Compact and less cracked gel films deposited on carbonized substrates form closed residual protection layers, which act as physical barrier to heat and mass transportation during the thermal decomposition. Similar results were reported by Miyafuji and Saka (1997), Shabir Mahr et al. (2012) and Wang et al. (2012). On the other hand, the change in the E_a of the WIC_{SiO_2} and WIC_{TiO_2} is different. The former exhibit higher E_a values during the advanced period of thermal decomposition (at conversion degrees >40%), whereas the latter shows higher E_a at the initial stage of degradation, at conversion degrees below 20%. This is probably due to the silica and titania deposition in the cell wall and in the cell lumens, respectively.

Seven decomposition temperatures (conversion degrees between 10% and 70%) at five heating rates (5, 10, 20, 30 and 40 K min^{-1}) were employed to find a correlation between the reaction order (n) and the decomposition temperature. The regression lines according to Avrami of W_{contr} and WICs are illustrated in Figure 4, and the corresponding data including the R^2 values (most of them higher than 0.99) are listed in Table 2. The data indicate the reaction orders: 0.51–0.57 (W_{contr}), 0.39–0.51 (WIC_{MTEOS}), 0.36–0.47 (WIC_{TEOS}) and 0.28–0.51 (WIC_{TTIP}). Vuthaluru (2004) and Gai et al. (2013) found reaction order values of wood waste, wheat straw and rice husks with 0.42, 0.52 and 0.539, respectively. However, the average value of the reaction order drastically decreased for all WICs. The additives discussed in the present paper not only changed the thermal decomposition path leading to the development of less combustible volatiles but also formed a closed barrier layer, which retards the thermal decomposition process.

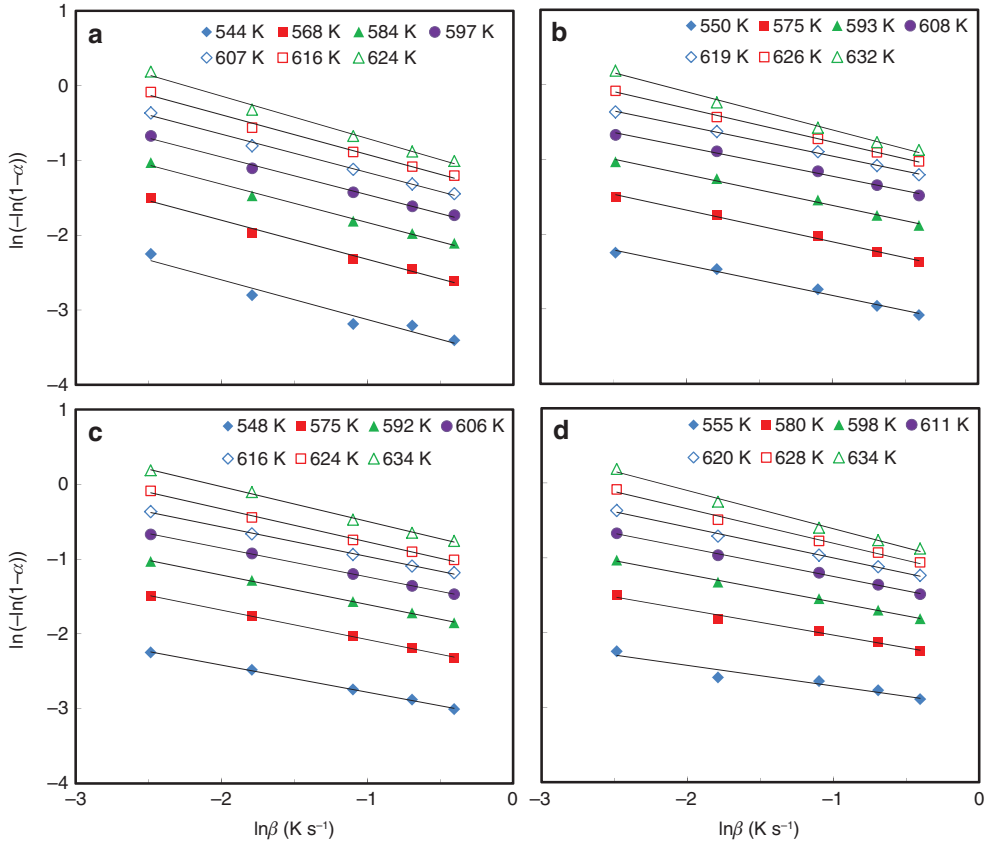

Figure 4: Illustration of the regression lines according to Avrami of W_{contr} and WICs.
Regression lines to the reaction order proposed by the Avrami theory for W_{contr} (a) and the WICs with WPG 20% prepared from MTEOS (b), TEOS (c) and TTIP (d).

Conclusions

The incorporation of SiO_2 or TiO_2 into wood by the sol-gel process is effective to improve the dimensional and thermal stability. According to SEM-EDX observations, most silica and titania are deposited in the cell wall and cell lumens, respectively. These deposits also result in higher E_a values at the late and early stages of thermal decomposition for the WIC_{SiO_2} and WIC_{TiO_2}, respectively. For the range of conversion rates (10–70%) investigated, the average E_a of all WICs with a 20% WPG (178–214 kJ mol^{-1}) was remarkably higher than that of the W_{contr} (156–168 kJ mol^{-1}), indicating their high thermal stability. Additionally, the reaction order was 0.51–0.57 (W_{contr}), 0.39–0.51 (WIC_{MTEOS}), 0.36–0.47 (WIC_{TEOS}) and 0.28–0.51 (WIC_{TTIP}).

Acknowledgments: This work was financially supported by a research grant from the Ministry of Science and Technology, Taiwan (MOST 105-2622-B-005-002-CC3).

Author contributions: All the authors have accepted responsibility for the entire content of this submitted manuscript and approved submission.
Research funding: The Ministry of Science and Technology of Taiwan (MOST 105-2622-B-005-002-CC3).
Employment or leadership: None declared.
Honorarium: None declared.

References

ASTM D1037-06a. Standard Test Methods for Evaluating Properties of Wood-Based Fiber and Particle Panel Materials. ASTM International, West Conshohocken, PA, 2006.

ASTM D2395-07a. Standard Test Methods for Specific Gravity of Wood and Wood-Based Materials. ASTM International, West Conshohocken, PA, 2007.

ASTM D4442-07. Standard Test Methods for Direct Moisture Content Measurement of Wood and Wood-Based Materials. ASTM International, West Conshohocken, PA, 2007.

Bartocci, P., Anca-Couce, A., Slopiecka, K., Nefkens, S., Evic, N., Retschitzegger, S., Barbanera, M., Buratti, C., Cotana, F., Bidini, G., Fantozzi, F. (2017) Pyrolysis of pellets made with biomass and glycerol: kinetic analysis and evolved gas analysis. Biomass Bioenerg. 97:11–19.

Beck, G., Strohbusch, S., Larnøy, E., Militz, H., Hill, C. (2018a) Accessibility of hydroxyl groups in anhydride modified wood as measured by deuterium exchange and saponification. Holzforschung 72:17–23.

Beck, G., Thybring, E.E., Thygesen, L.G., Hill, C. (2018b) Characterization of moisture in acetylated and propionylated radiata pine using low-field nuclear magnetic resonance (LFNMR) relaxometry. Holzforschung 72:225–233.

Boonstra, M.J., Tjeerdsma, B. (2006) Chemical analysis of heat treated softwoods. Eur. J. Wood Prod. 64:204–211.

Brown, M.E., Maciejewski, M., Vyazovkin, S., Nomen, R. Sempere, J., Burnham, A. (2000) Computational aspects of kinetic analysis. Part A: the ICTAC kinetics project-data, methods and results. Thermochim. Acta 355:125–143.

Chandrasekaran, A., Ramachandran, S., Subbiah, S. (2017) Determination of kinetic parameters in the pyrolysis operation and thermal behavior of *Prosopis juliflora* using thermogravimetric analysis. Bioresource Technol. 233:413–422.

Chaouch, M., Pétrissans, M., Pétrissans, A., Gérardin, P. (2010) Use of wood elemental composition to predict heat treatment intensity and decay resistance of different softwood and hardwood species. Polym. Degrad. Stabil. 95:2255–2259.

Chi, F.K. (1983) Carbon-containing monolithic glasses via the sol-gel process. Ceram. Eng. Sci. Proc. 4:704–717.

Gai, C., Dong, Y., Zhang, T. (2013) The kinetic analysis of the pyrolysis of agricultural residue under non-isothermal conditions. Bioresource Technol. 127:298–305.

Gao, J., Kim, J.S., Terziev, N., Daniel, G. (2016) Decay resistance of softwoods and hardwoods thermally modified by the Thermovouto type thermo-vacuum process to brown rot and white rot fungi. Holzforschung 70:877–884.

Gholamiyan, H., Tarmian, A., Ranjbar, Z., Abdulkhani, A., Azadfallah, M., Mai, C. (2016) Silane nanofilm formation by sol-gel processes for promoting adhesion of waterborne and solventborne coatings to wood surface. Holzforschung 70:429–437.

Hill, C.A.S. Wood modification: chemical, thermal and other process. John Wiley & Sons, Chichester, UK, 2006.

Himmel, S., Mai, C. (2016) Water vapour sorption of wood modified by acetylation and formalisation – analysed by a sorption kinetics model and thermodynamic considerations. Holzforschung 70:203–213.

Hübert, T., Unger, B., Bücker, M. (2010) Sol-gel derived TiO_2 wood composites. J. Sol-Gel Sci. Technol. 53:384–389.

Hung, K.-C., Wu, J.-H. (2017) Characteristics and thermal decomposition kinetics of wood-SiO_2 composites derived by the sol-gel process. Holzforschung 71:233–240.

Hung, K.-C., Yang, C.-N., Yang, T.-C., Wu, T.-L., Chen, Y.-L., Wu J.-H. (2017) Characterization and thermal stability of acetylated slicewood production by alkali-catalyzed esterification. Materials 10:393.

Innocenzi, P., Abdirashid, M.O., Guglielmi, M. (1994) Structure and properties of sol-gel coatings from methyltriethoxysilane and tetraethoxysilane. J. Sol-Gel Sci. Technol. 3:47–55.

Kamiya, K., Yoko, T., Tanaka, K., Takeuchi, M. (1990) Thermal evolution of gels derived from $CH_3Si(OC_2H_5)_3$ by the sol-gel method. J. Non-Cryst. Solids 121:182–187.

Kartal, S.N., Yoshimura, T., Imamura, Y. (2004) Decay and termite resistance of boron-treated and chemically modified wood by in situ co-polymerization of allyl glycidyl ether (AGE) with methyl methacrylate (MMA). Int. Biodeterior. Biodegrad. 53:111–117.

Kartal, S.N., Yoshimura, T., Imamura, Y. (2009) Modification of wood with Si compounds to limit boron leaching from treated wood and to increase termite and decay resistance. Int. Biodeterior. Biodegrad. 63:187–190.

Lee, X.J., Lee, L.Y., Gan, S., Thangalazhy-Gopakumar, S., Ng, H.K. (2017) Biochar potential evaluation of palm oil wastes through slow pyrolysis: thermochemical characterization and pyrolytic kinetic studies. Bioresource Technol. 236:155–163.

Li, Y.F., Dong, X.Y., Liu, Y.X., Li, J., Wang, F.H. (2011) Improvement of decay resistance of wood via combination treatment on wood cell wall: swell-bonding with maleic anhydride and graft copolymerization with glycidyl methacrylate and methyl methacrylate. Int. Biodeter. Biodegr. 67:1087–1094.

Li, Y., Du, L., Kai, C., Huang, R., Wu, Q. (2013) Bamboo and high density polyethylene composite with heat-treated bamboo fiber: thermal decomposition properties. Bioresources 8:900–912.

Ma, Z., Chen, D., Gu, J., Bao, B., Zhang, Q. (2015) Determination of pyrolysis characteristics and kinetics of palm kernel shell using TGA–FTIR and model-free integral methods. Energ. Convers. Manage. 89:251–259.

Miyafuji, H., Saka, S. (1997) Fire-resistant properties in several TiO_2 wood-inorganic composites and their topochemistry. Wood Sci. Technol. 31:449–455.

Miyafuji, H., Saka, S. (2001) Na_2O-SiO_2 wood-inorganic composites prepared by the sol-gel process and their fire-resistant properties. J. Wood Sci. 47:483–489.

Miyafuji, H., Kokaji, H., Saka, S. (2004) Photostable wood-inorganic composites prepared by the sol-gel process with UV absorbent. J. Wood Sci. 50:130–135.

Moghaddam, M., Wålinder, M.E.P., Claesson, P.M., Swerin, A. (2016) Wettability and swelling of acetylated and furfurylated wood analyzed by multicycle Wilhelmy plate method. Holzforschung 70:69–77.

Nocuń, M, Gajerski, R., Siwulski S. (2005) Thermal decomposition of silica-methyltrimethoxysilane hybrid glasses studied by mass spectrometry. Opt. Appl. 35:901–906.

Poletto, M., Zattera, A.J., Santana, R.M.C. (2012) Thermal decomposition of wood: kinetics and degradation mechanisms. Bioresource Technol. 126:7–12.

Pries, M., Mai, C. (2013) Fire resistance of wood treated with a cationic silica sol. Eur. J. Wood Prod. 71:237–244.

Qin, C., Zang, W. (2012) Antibacterial properties of titanium alkoxide/poplar wood composite prepared by sol-gel process. Mater. Lett. 89:101–103.

Rowell, R.M., LeVan-Green, S.L. Handbook of wood chemistry and wood composites. Taylor & Francis, New York, 2005.

Saka, S., Yakake, Y. (1993) Wood-inorganic composites prepared by sol-gel process III. Chemically-modified wood-inorganic composites. Mokuzai Gakkaishi 39:308–314.

Saka, S., Ueno, T. (1997) Several SiO_2 wood-inorganic composites and their fire-resisting properties. Wood Sci. Technol. 31:457–466.

Saka, S., Sasaki, M., Tanahashi, M. (1992) Wood-inorganic composites prepared by sol-gel processing I. Wood-inorganic composites with porous structure. Mokuzai Gakkaishi 30:1043–1049.

Sakka, S., Miyafuji, H. Handbook of Sol-Gel Science and Technology: Processing, Characterization, and Applications. Volume III: Applications of Sol-Gel Technology. Kluwer Academic Publishers, Boston, 2005.

Shabir Mahr, M., Hübert, T., Schartel, B., Bahr, H., Sabel, M., Militz, H. (2012) Fire retardancy effects in single and double layered sol-gel derived TiO_2 and SiO_2-wood composites. J. Sol-Gel Sci. Technol. 64:452–464.

Shabir Mahr, M., Hübert, T., Stephan, I., Bücker, M., Militz, H. (2013) Reducing copper leaching from treated wood by sol-gel derived TiO_2 and SiO_2 depositions. Holzforschung 67:429–435.

Strandberg, A., Holmgren, P., Broström, M. (2017) Predicting fuel properties of biomass using thermogravimetry and multivariate data analysis. Fuel Process. Technol. 156:107–112.

Tshabalala, M.A., Libert, R., Schaller, C.M. (2011) Photostability and moisture uptake properties of wood veneers coated with a combination of thin sol-gel films and light stabilizers. Holzforschung 65:215–220.

Vuthaluru, H.B. (2004) Investigations into the pyrolytic behavior of coal/biomass blends using thermogravimetric analysis. Bioresource Technol. 92:187–195.

Wang, X., Liu, J., Chai, Y. (2012) Thermal, mechanical, and moisture absorption properties of wood-TiO_2 composites prepared by a sol-gel process. Bioresources 7:893–901.

Yao, F., Wu, Q., Lei, Y., Guo, W., Xu, Y. (2008) Thermal decomposition kinetics of natural fibers: activation energy with dynamic thermogravimetric analysis. Polym. Degrad. Stabil. 93:90–98.

Yoon, J.D., Park, K.Y., Jang, H.D. (2003) Comparison of titania particles between oxidation of titanium tetrachloride and thermal decomposition of titanium tetraisopropoxide. Aerosol Sci. Technol. 37:621–627.

Zaharescu, M., Jitianu, A., Brãileanu, A., Madarász, J., Novák, C.S., Pokol, G. (2003) Composition and thermal stability of SiO_2-based hybrid materials TEOS-MTEOS system. J. Therm. Anal. Calorim. 71:421–428.

Zhang, X., Lei, H., Zhu, L., Zhu, X., Qian, M., Yadavalli, G., Wu, J., Chen, S. (2016) Thermal behavior and kinetic study for catalytic co-pyrolysis of biomass with plastics. Bioresource Technol. 220:233–238.